The Astrophysical Journal, 631:163–168, 2005 September 20

MID-INFRARED SELECTION OF ACTIVE GALAXIES

Daniel Stern,[1] Peter Eisenhardt,[1] Varoujan Gorjian,[1] Christopher S. Kochanek,[2] Nelson Caldwell,[3] Daniel Eisenstein,[4] Mark Brodwin,[1] Michael J. I. Brown,[5,6] Richard Cool,[4] Arjun Dey,[6] Paul Green,[3] Buell T. Jannuzi,[6] Stephen S. Murray,[3] Michael A. Pahre,[3] and S. P. Willner[3]

Received 2004 October 21; accepted 2005 June 2

ABSTRACT

Mid-infrared photometry provides a robust technique for identifying active galaxies. While the ultraviolet to mid-infrared ($\lambda \lesssim 5$ μm) continuum of stellar populations is dominated by the composite blackbody curve and peaks at approximately 1.6 μm, the ultraviolet to mid-infrared continuum of active galactic nuclei (AGNs) is dominated by a power law. Consequently, with a sufficient wavelength baseline, one can easily distinguish AGNs from stellar populations. Mirroring the tendency of AGNs to be *bluer* than galaxies in the ultraviolet, where galaxies (and stars) sample the blue, rising portion of stellar spectra, AGNs tend to be *redder* than galaxies in the mid-infrared, where galaxies sample the red, falling portion of the stellar spectra. We report on *Spitzer Space Telescope* mid-infrared colors, derived from the IRAC Shallow Survey, of nearly 10,000 spectroscopically identified sources from the AGN and Galaxy Evolution Survey. On the basis of this spectroscopic sample, we find that simple mid-infrared color criteria provide remarkably robust separation of active galaxies from normal galaxies and Galactic stars, with over 80% completeness and less than 20% contamination. Considering only broad-lined AGNs, these mid-infrared color criteria identify over 90% of spectroscopically identified quasars and Seyfert 1 galaxies. Applying these color criteria to the full imaging data set, we discuss the implied surface density of AGNs and find evidence for a large population of optically obscured active galaxies.

Subject headings: cosmology: observations — galaxies: formation

1. INTRODUCTION

The dominant sources of energy production in the universe are fusion in stars and gravitational accretion onto supermassive black holes. The tight correlation between nuclear black hole mass and bulge mass (e.g., Magorrian et al. 1998; Tremaine et al. 2002) implies the processes are intimately connected. However, identifying an unbiased census of black holes in the universe remains challenging, hampering our ability to fully probe this connection. The spectrum of the X-ray background, which is significantly harder than that of bright, unobscured quasars, implies that a large population of heavily obscured active galactic nuclei (AGNs) exists. Resolving the X-ray background was one of the primary motivators for the *Chandra X-Ray Observatory* and *XMM-Newton*, and these satellites have successfully identified a population of high-redshift, heavily obscured, luminous "type 2 quasars"[7] (e.g., Stern et al. 2002b; Norman et al. 2002), as well as a significant population of X-ray–bright, optically normal galaxies (e.g., Barger et al. 2001; Hornschemeier et al. 2001; Stern et al. 2002a). Notably, while the deepest surveys with *Chandra* and *XMM-Newton* have resolved $\gtrsim$90% of the 0.5–2 keV X-ray background, the resolved fraction falls at higher energies, with only $\sim$50% of the background resolved at 10 keV (Worsley et al. 2005), implying that a significant population of AGNs remain unidentified.

The *Spitzer Space Telescope* (Werner et al. 2004) also provides another valuable probe of AGN demographics. The obscuring dust that hides AGNs from ultraviolet, optical, and soft X-ray surveys should be a strong, largely isotropic emitter in the mid- to far-infrared ($\lambda \gtrsim 20$ μm). Furthermore, normal and active galaxies have different spectral energy distributions (SEDs) at shorter wavelengths ($\lambda \lesssim 10$ μm): the composite blackbody spectra of the stellar population of normal galaxies produce an SED that peaks at approximately 1.6 μm, while quasars have a roughly power-law SED, $f_\nu \propto \nu^{-\alpha}$. One of the early, traditional techniques to identify quasars relies on identifying sources with an ultraviolet excess, targeting sources whose SED does not plummet on the blue side of the stellar peak (e.g., Schmidt & Green 1983). Although fruitful, this technique fails in two cases: (1) obscured quasars preferentially suffer attenuation of their ultraviolet flux and (2) high-redshift quasars disappear from the ultraviolet due to absorption from the Lyman forests.

By contrast, we seek to exploit the manifold improvement in mid-infrared sensitivity afforded by *Spitzer* to target sources having SEDs that do not decline on the *red* side of the stellar peak. This provides an approach to identifying AGNs that is relatively insensitive to extinction by dust or gas, and it has been demonstrated with a variety of instrumentation, including the Two Micron All-Sky Survey (e.g., Cutri et al. 2001; Glikman et al. 2004), the *Infrared Space Observatory* (e.g., Laurent et al. 2000; Haas et al. 2004), and *Spitzer* (e.g., Lacy et al. 2004; Sajina et al. 2005; Hatziminaoglou et al. 2005).

We present here a study of the mid-infrared colors of 800 spectroscopically confirmed AGNs from the 9 deg^2 Boötes field of the NOAO Deep Wide-Field Survey (NDWFS; Jannuzi & Dey 1999; A. Dey et al. 2005, in preparation; B. T. Jannuzi et al. 2005, in preparation). The mid-infrared colors are from the

[1] Jet Propulsion Laboratory, California Institute of Technology, 4800 Oak Grove Drive, MS 169-506, Pasadena, CA 91109; stern@zwolfkinder.jpl.nasa.gov.
[2] Department of Astronomy, Ohio State University, Columbus, OH 43210.
[3] Steward Observatory, University of Arizona, 933 North Cherry Avenue, Tucson, AZ 85721.
[4] Harvard-Smithsonian Center for Astrophysics, 60 Garden Street, Cambridge, MA 02138.
[5] Princeton University Observatory, Princeton, NJ 08544.
[6] National Optical Astronomy Observatory, 950 North Cherry Avenue, Tucson, AZ 85719.
[7] Throughout we distinguish type 1 and type 2 AGNs based solely on their optical spectra. Type 1 AGNs are defined to be sources with broad emission lines. Type 2 AGNs are defined to be sources lacking broad emission lines but with high-ionization, narrow emission lines indicative of AGN activity.

Infrared Array Camera (IRAC) Shallow Survey (Eisenhardt et al. 2004), a guaranteed-time program with *Spitzer*. The spectroscopy comes from the AGN and Galaxy Evolution Survey (AGES; C. Kochanek et al. 2005, in preparation). AGES includes redshifts and spectral classifications for nearly 10,000 normal galaxies and nearly 1000 AGNs. On the basis of this spectroscopic sample, we show that mid-infrared photometry provides a robust technique for identifying AGNs. Using empirical color criteria to isolate AGNs, we use the entire IRAC Shallow Survey to study the surface density of active galaxies and evaluate the efficacy of mid-infrared selection of AGNs. A coordinated paper discusses the mid-infrared colors of X-ray sources in this field (V. Gorjian et al. 2005, in preparation).

Section 2 briefly summarizes the two surveys used. Section 3 describes the mid-infrared properties of the spectroscopically identified sources, followed by a discussion of mid-infrared selection of AGNs in § 4. The results are summarized in § 5. Unless otherwise noted, all magnitudes refer to the Vega system.

2. SURVEY DATA

2.1. *IRAC Shallow Survey*

IRAC (Fazio et al. 2004) is a four-channel instrument on *Spitzer* that provides simultaneous broadband images at 3.6, 4.5, 5.8, and 8.0 μm with unprecedented sensitivity. The IRAC shallow survey, a guaranteed-time observation program of the IRAC instrument team, covers 8.5 deg^2 in the NDWFS Boötes field with three or more 30 s exposures per position. Eisenhardt et al. (2004) present an overview of the survey design, reduction, calibration, and initial results. The survey identifies $\approx$270,000, 200,000, 27,000, and 26,000 sources brighter than 5 σ limits of 12.3, 15.4, 76, and 76 μJy at 3.6, 4.5, 5.8, and 8.0 μm, respectively, where throughout IRAC magnitudes were measured in 6″ diameter apertures and corrected to total magnitudes assuming sources are unresolved at the 1.″66–1.″98 resolution of IRAC (Fazio et al. 2004). The corresponding magnitude limits are 18.4, 17.7, 15.5, and 14.8 mag.

2.2. *AGN and Galaxy Evolution Survey*

AGES (C. Kochanek et al. 2005, in preparation) is a wide-field redshift survey in the NDWFS Boötes field using Hectospec (Fabricant et al. 1998), a new, multiobject fiber spectrograph at the MMT Observatory. For the 2004 observing season, AGES targeted sources from the NDWFS catalog (B. T. Jannuzi et al. 2005, in preparation) with $R < 21.5$, with priorities based on the multiwavelength photometry available. AGES observed (1) all extended sources with $R \leq 19.2$, (2) a randomly selected 20% of extended sources with $19.2 < R \leq 20$, (3) all $R \leq 20$ extended sources with IRAC 3.6, 4.5, 5.8, and 8.0 μm magnitudes less than or equal to 15.2, 15.2, 14.7, and 13.2, respectively, and (4) fainter sources with a strong selection bias in favor of counterparts to X-ray sources from *Chandra* imaging of the field (Murray et al. 2005; Brand et al. 2005; Kenter et al. 2005), radio sources from the FIRST survey (Becker et al. 1995), and 24 μm sources with nonstellar $J-$ [24] colors, where the 24 μm data derive from the Multiband Imaging Photometer for *Spitzer* (Rieke et al. 2004) observations of the field (E. Le Floc'h et al. 2005, in preparation). C. Kochanek et al. (2005, in preparation) provide a more detailed description of the target selection. In particular, point sources (in the B_W-, R-, or I-band images of NDWFS) were selected against *unless* they were associated with $R \leq 21.5$ counterparts to X-ray, radio, or 24 μm sources.

We use the AGES version 1.11 catalog, containing all AGES spectra taken in 2004. The redshift catalog, created by N. Caldwell, P. Green, and C. Kochanek, includes 10,452 sources with confident redshifts. Spectra were initially assigned to three categories: stars, galaxies with broad emission lines, and galaxies without broad emission lines. All broad-line sources are obvious AGNs, e.g., quasars and Seyfert 1 galaxies. The galaxies without broad lines were further separated, using conservative emission line diagnostics,[8] into narrow-line AGNs and normal (optically inactive) galaxies. The AGES sample with well-determined redshifts is composed of 9394 optically inactive galaxies, 733 broad-lined AGNs, 118 narrow-lined AGNs, and 207 Galactic stars. Most of the stars are F stars, targeted by AGES for spectrophotometric calibration. Matching AGES sources with the 3.6 μm–selected IRAC Shallow Survey catalog by requiring $\leq 2''$ separation between the IRAC mid-infrared source and NDWFS optical source and ≥ 5 σ detections in all four IRAC bands leads to a restricted spectroscopic sample of 4693 sources comprising 3959 normal galaxies, 576 broad-lined AGNs, 99 narrow-lined AGNs, and 59 stars. For some analyses, we only require IRAC 5 σ detections in the two bluest IRAC bands; the matched catalog for this subsample contains 9432 sources comprising 8460 normal galaxies, 696 broad-lined AGNs, 104 narrow-lined AGNs, and 172 stars.

3. MID-INFRARED PROPERTIES OF AGNs

Figure 1 presents an IRAC color-color diagram for the AGES sample, with symbols denoting spectroscopic classification. Solely on the basis of photometric data, Eisenhardt et al. (2004) noted a vertical spur in the [3.6]–[4.5] versus [5.8]–[8.0] color-color diagram (see Fig. 5*c* of that paper) and suggested that it may be associated with AGNs since a large fraction of those sources are spatially unresolved at 3.6 μm. These spectroscopic results confirm that suggestion: mid-infrared colors clearly separate AGNs from both stars and galaxies in the AGES sample. In order to achieve a physical understanding of Figure 1, we now discuss the mid-infrared properties of stars, galaxies, and AGNs.

Galactic stars primarily reside in a restricted locus in mid-infrared color space, corresponding to the Rayleigh-Jeans tail of the blackbody spectrum: stellar photospheres have approximately zero color in the Vega system. The majority of the spectroscopically confirmed stars in the AGES sample confirm this expectation. The AGES sample also includes several stars that reside far from the stellar locus, showing mid-infrared excesses in the IRAC bands. Such stars likely host cooler circumstellar material in the form of post–asymptotic giant branch shells or circumstellar disks. A more detailed treatment of the Galactic color-space outliers is deferred to a future publication.

Because of its R-band magnitude limit, AGES identifies normal galaxies out to $z \sim 0.6$. As seen in Figures 1 and 2, inactive galaxies at $z \lesssim 1$ span a relatively modest range in the bluest IRAC color combination, $-0.2 \lesssim$ [3.6]–[4.5] $\lesssim 0.5$. For reference, we show the color evolution of two galaxy templates from Devriendt et al. (1999): M82 is a starburst galaxy with strong polycyclic aromatic hydrocarbon (PAH) features, while VCC 1003 (=NGC 4429), a Virgo Cluster S0/Sa galaxy, is not actively forming stars. At $0.2 \lesssim z \lesssim 0.5$, galaxies appear redder in [3.6]–[4.5] due to a combination of the 3.3 μm PAH feature shifting through the IRAC 4.5 μm band (for actively star-forming galaxies) and the deep 2.35–2.5 μm CO absorption due to red supergiants (e.g., Förster Schreiber 2000) shifting through the IRAC 3.6 μm band (for older stellar populations). At $z \gtrsim 1$,

[8] Galaxies without broad lines were classified type 2 AGNs if they showed detectable [Ne v] λ3426 emission (usable for $z > 0.15$) or (for $z < 0.35$) if [N ii] λ6583/H$\alpha > 2$, [O iii] λ5007/H$\beta > 2$, and [O i] λ6300 were detected.

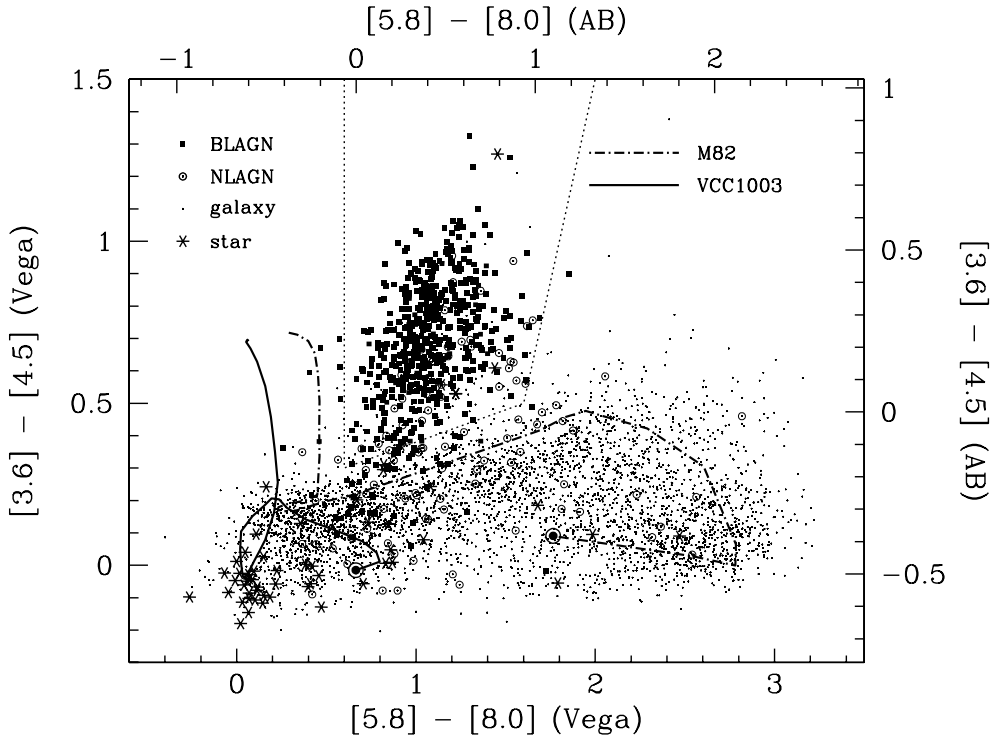

FIG. 1.—IRAC colors of spectroscopically identified objects from the AGES survey of the Boötes field. Axes indicate both the Vega and AB magnitude systems. Spectral classification of sources is noted in the upper left. The $0 \leq z \leq 2$ color tracks for two nonevolving galaxy templates from Devriendt et al. (1999) are illustrated; dark bull's eyes indicate $z = 0$. M82 is a starburst galaxy, while VCC 1003 (=NGC 4429) is an S0/Sa galaxy with a star formation rate approximately 4000 times lower. The dotted line empirically separates active galaxies from Galactic stars and normal galaxies.

which lies beyond the redshift range in which AGES is sensitive to normal galaxies, the templates redden once again as the 1.6 μm maximum in the photospheric emission from stellar populations shifts from the 3.6 μm IRAC band to the 4.5 μm IRAC band.

Galaxies at $z \lesssim 0.6$ span a large range of color in the reddest IRAC color combination, $0 \lesssim [5.8]–[8.0] \lesssim 3$ (Figs. 1 and 3), due to the 6.2 and 7.7 μm PAH features in actively star-forming galaxies shifting through the IRAC 8.0 μm band. The 6.2 and 7.7 μm PAH features are much stronger than the 3.3 μm PAH feature, explaining why the observed range of [5.8]–[8.0] colors for normal galaxies is much more expansive than the observed [3.6]–[4.5] color range. The 3.3 μm PAH feature later causes a modest, broad red bump in galaxy template [5.8]–[8.0] colors at $z \approx 1.3$. At $z \gtrsim 2$, the 1.6 μm bump causes the

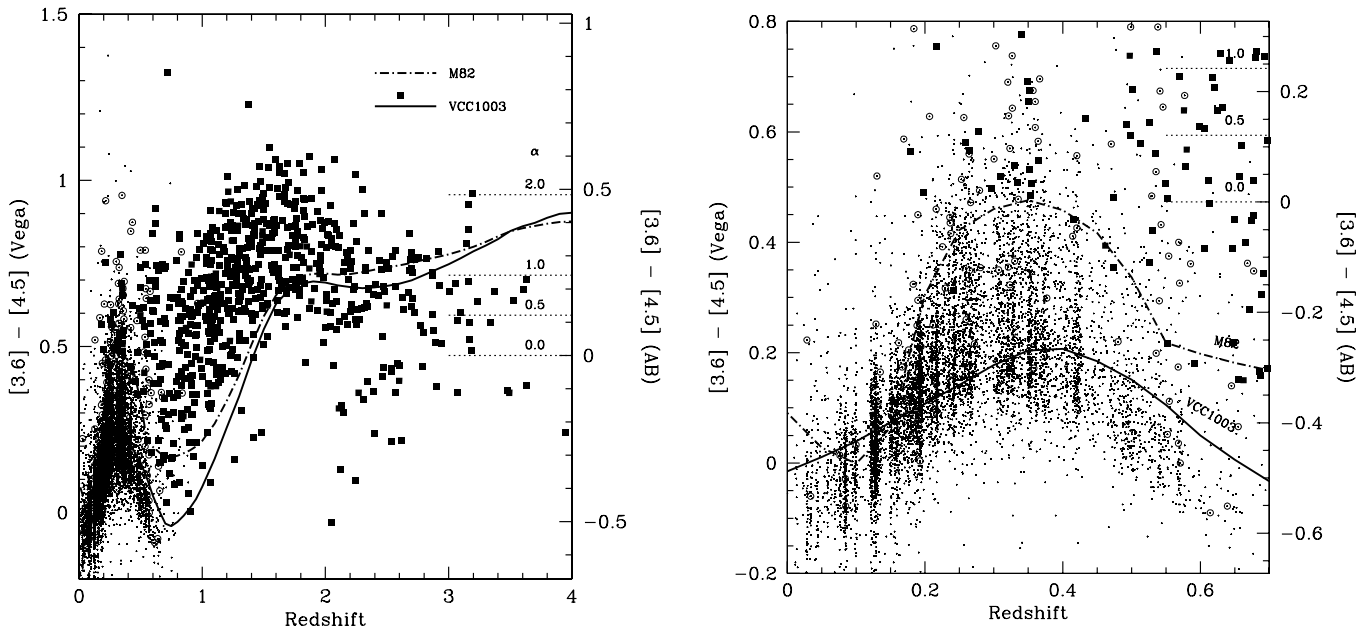

FIG. 2.—IRAC [3.6]–[4.5] color evolution of galaxies, AGNs, and galaxy templates. Symbols are the same as in Fig. 1. The left panel shows the full observed redshift range, highlighting the modest average color evolution of AGNs. The right panel shows $z \leq 0.7$, highlighting the color evolution of normal galaxies. Horizontal dotted lines illustrate the expected mid-IR color of power-law SEDs, $f_\nu \propto \nu^{-\alpha}$, for $0.5 < \alpha < 2.0$.

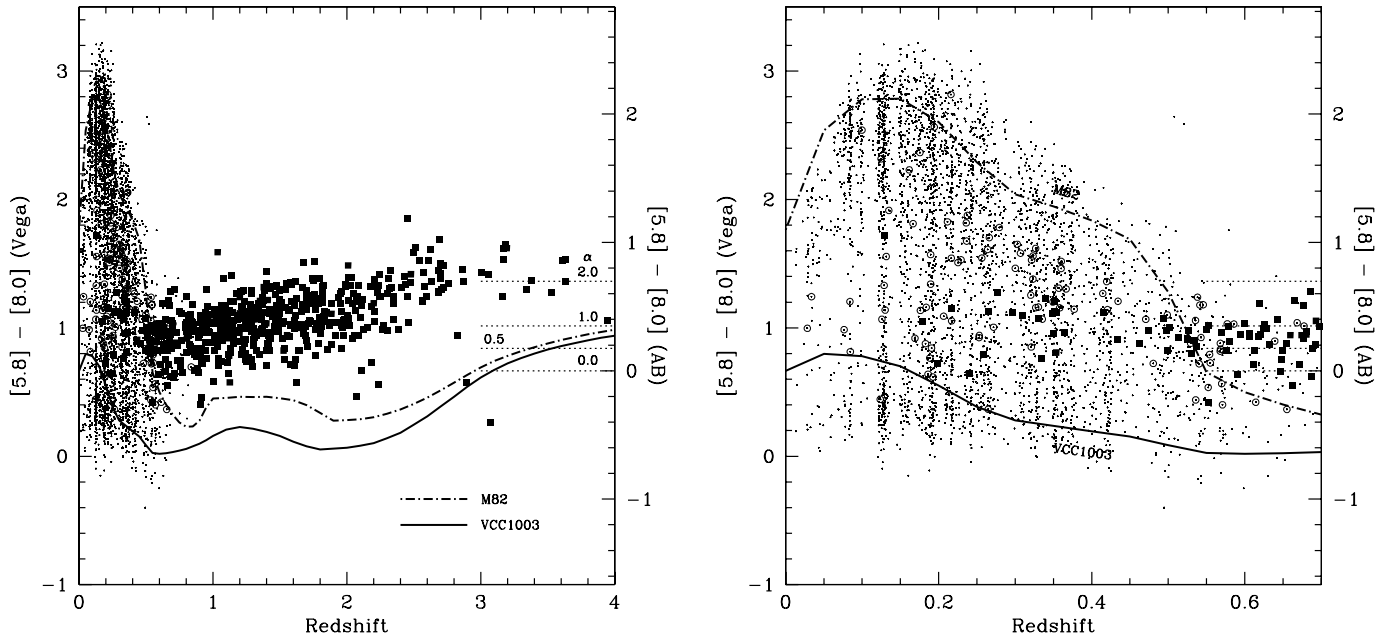

FIG. 3.—IRAC [5.8]–[8.0] color evolution of galaxies, AGNs, and galaxy templates. Symbols are the same as in Figs. 1 and 2. The left panel shows the full observed redshift range, highlighting the modest average color evolution of AGNs. The right panel shows $z \leq 0.7$, highlighting the color evolution of normal galaxies. Horizontal dotted lines illustrate the expected mid-IR color of power-law SEDs, $f_\nu \propto \nu^{-\alpha}$.

galaxy templates to redden once again. As seen in Figures 1–3, the Devriendt et al. (1999) M82 and VCC 1003 templates approximately bound the observed range of AGES galaxies in both IRAC color-color space and in IRAC color-redshift space.

The isolation of broad-lined AGNs in mid-infrared color-color space is the most dramatic feature of Figure 1. While stars are generally restricted to a single locus of zero color and $z \lesssim 0.6$ galaxies define a horizontal swath in Figure 1, broad-lined AGNs create a vertical branch in the diagram. This characteristic property is easily understood. First, the lack of strong PAH emission in powerful AGNs restricts their observed [5.8]–[8.0] colors. Second, since the $\lambda \lesssim 5$ μm flux of AGNs is dominated by power-law emission rather than a composite stellar spectrum that peaks at $\approx$1.6 μm, the [3.6]–[4.5] color of AGNs is significantly redder than that of low-redshift galaxies. The tendency of AGNs to be *redder* than galaxies in the mid-infrared, where galaxies sample the red, falling side of the composite blackbody stellar spectrum, mirrors the tendency of AGNs to be *bluer* than galaxies (and stars) in the ultraviolet, where we are sampling the blue, rising side of the stellar spectrum.

The power-law nature of quasar SEDs is consistent with previous studies at optical wavelengths. Vanden Berk et al. (2001) present a composite quasar spectrum derived from over 2200 Sloan Digital Sky Survey (SDSS) spectra. Fitting the continuum at rest-frame wavelengths $\lambda\lambda_0$ 1300–5000 Å with a power law, $f_\nu \propto \nu^{-\alpha}$, Vanden Berk et al. (2001) find an average spectral slope $\alpha = 0.44 \pm 0.1$, comparable to the $\alpha = 0.57 \pm 0.33$ derived by Pentericci et al. (2003) from a sample of 45 high-redshift SDSS quasars imaged in the near-infrared. IRAC observations of AGNs from the AGES survey suggest a modest steepening of the average quasar spectrum at longer wavelengths. Considering the 696 AGES broad-lined AGNs with robust ($\geq 5\,\sigma$) data in the bluest IRAC passbands, the sigma-clipped average [3.6]–[4.5] color is 0.65 ± 0.20 (Vega), corresponding to a spectra index $\alpha = 0.73 \pm 0.84$. Considering the 576 AGES broad-lined AGNs with robust photometry in all four IRAC bands, the sigma-clipped average [3.6]–[8.0] color is 2.53 ± 0.46 (Vega), corresponding to a spectra index $\alpha = 1.07 \pm 0.53$. AGNs tend to be redder in [3.6]–[4.5] for $z > 1$ (Fig. 2) and in [5.8]–[8.0] for $z > 2$ (Fig. 3). The color change suggests that the 1.6 μm stellar bump contributes to the mid-infrared flux. C. Kochanek et al. (2005, in preparation) present a more detailed treatment of the composite AGES AGN spectrum in the mid-infrared, derived from a principal component analysis of the IRAC photometry.

The narrow-lined AGNs in the AGES sample appear in both the region of IRAC color-color space dominated by galaxies and the region dominated by broad-lined AGNs. The narrow-lined AGN sample apparently includes sources whose mid-infrared flux can be dominated by either stellar emission or emission associated with a powerful active nucleus.

4. MID-INFRARED SELECTION OF AGNs

We adopt the following empirical criteria to separate active galaxies from other sources in the AGES spectroscopic sample described above (Fig. 1, *dotted line*):

$$([5.8]-[8.0]) > 0.6 \wedge ([3.6]-[4.5]) > 0.2\cdot([5.8]-[8.0]) + 0.18$$
$$\wedge ([3.6]-[4.5]) > 2.5\cdot([5.8]-[8.0]) - 3.5,$$

where $\wedge$ is the logical AND operator. The left boundary protects against fainter, higher redshift galaxies and is not critical for relatively shallow surveys such as AGES. The right boundary merely approximates the outer range of AGN colors. Considering Figure 2, we caution that these color criteria may preferentially omit AGNs at $z \approx 0.8$ and 2. Of a total of 681 sources that reside in this portion of mid-infrared color-color space in Figure 1, 522 (77%) are spectroscopically classified as broad-lined AGNs, 40 (6%) are spectroscopically classified as narrow-lined AGNs, 113 (17%) are spectroscopically classified as galaxies, and 6 (1%) are spectroscopically classified as stars. Of all 576 AGES sources spectroscopically classified as broad-lined AGNs and having good four-band IRAC data, 522 (91%) meet these mid-infrared color criteria. Of the 99 AGES sources spectroscopically classified as narrow-lined AGNs and having

good four-band IRAC data, 40 (40%) meet these mid-infrared color criteria. Furthermore, less than 3% of the nearly 4000 AGES normal galaxies would be (mis-)classified as AGNs using these mid-infrared criteria. Some sources classified as normal galaxies by AGES based on their optical spectra likely still host an active, supermassive black hole: *Chandra* has identified a large population of luminous X-ray sources ($L_{2-10\,\mathrm{keV}} \gtrsim 10^{42}$ ergs s^{-1}) with apparently normal optical spectra (e.g., Stern et al. 2002a). Similar sources might be below the existing X-ray limits for the Boötes field (Murray et al. 2005) but still be correctly identified as AGNs by *Spitzer*.

Optical surveys find an increasing number of quasars as flux limits become fainter—the SDSS finds 15 quasars deg^{-2} to $i^* = 19.1$ (Richards et al. 2002), the 2dF Quasar Redshift Survey finds 35 quasars per deg^2 to $b_J = 20.85$ (Croom et al. 2004), and the COMBO-17 survey AGN luminosity function implies approximately 65 quasars per deg^2 to $R = 21$ (Wolf et al. 2003). Using the mid-infrared selection criteria on the full IRAC Shallow Survey photometric catalog (ver. 1.1) of 14,099 non-saturated sources with $\geq 5\,\sigma$ detections in all IRAC bands, there are 2014 AGN candidates over the 8.06 deg^2 of the NDWFS with four-band IRAC coverage. This translates to an approximate surface density of 275 AGN candidates per deg^2 to an 8.0 μm flux limit of 76 μJy, where we have applied a modest incompleteness correction to account for the 9% of type 1 AGNs in AGES that lie outside our mid-IR color criteria. Since many (60%) of the narrow-lined AGNs identified by AGES are not recovered from the mid-IR color criteria, this surface density should be considered a lower limit. For a spectral index $\alpha = 0.75$ (§ 3), the mid-infrared depth of the IRAC images correspond to $R \approx 21$. The significantly higher surface density of IRAC-selected AGNs relative to optically selected AGNs of comparable mid-infrared flux implies a sizable population of obscured quasars with attenuation of their observed optical light.

The relatively shallow ($R \leq 21.5$) limit of the AGES spectroscopic follow-up may bias our results: AGES only identifies galaxies up to $z \lesssim 0.6$, while the Devriendt et al. (1999) SEDs plotted in Figure 1 encroach on our AGN selection criteria at $z \approx 1.4$. Some of the sources classified as AGNs based on their IRAC colors are likely moderate-redshift galaxies, fainter than the AGES optical spectroscopic limits. However, our implied AGN surface density is below that predicted by models of mid-infrared AGN number counts. For $\Omega_\Lambda = 0.7$, $\Omega_m = 0.3$, and $H_0 = 70$ km s^{-1} Mpc^{-1}, Andreani et al. (2003) predict $\sim 9 \times 10^4$ AGNs deg^{-2} with an 8 μm flux higher than 100 μJy, while Treister et al. (2004) predict only $\sim$1250 AGNs deg^{-2} to the same flux limit. The large discrepancy is due to differences in the assumed evolution of the AGN luminosity functions. Since the IRAC Shallow Survey only detects $\sim$3000 *sources* deg^{-2} with an 8 μm flux higher than 76 μJy, the Andreani et al. (2003) predictions are clearly high.

5. SUMMARY

The IRAC Shallow Survey includes 4693 sources with detections in all four IRAC bands and with well-determined spectroscopic redshifts from AGES version 1.11. Among these are 576 type 1 and 99 type 2 spectroscopically confirmed AGNs. Simple mid-infrared color criteria select over 90% of the spectroscopically identified type 1 AGNs and 40% of the type 2 AGNs. Of the AGES sources that fall within the color criteria, only 17% are not spectroscopically identified as AGNs. Many of these may host an active nucleus either hidden by dust or overpowered by stellar emission from the host galaxy (e.g., Moran et al. 2002). Simple mid-infrared selection criteria imply a surface density of 275 AGN candidates deg^{-2} to an 8 μm flux limit of 76 μJy, nearly quadruple the surface density inferred from optical surveys to this flux limit. Many of these sources are quite optically faint ($R \gtrsim 24$) and may be of the obscured, *type 2* variety, which are implied by unified models of AGNs and are invoked by models of the X-ray background. We show that the *Spitzer Space Telescope* is a powerful tool for studying AGN demographics; *Spitzer* will help identify a less-biased sample of supermassive black holes in the universe, allowing us to probe the interconnection of fusion-driven and accretion-driven energy production over cosmic history.

We thank M. Ashby, J. Hora, and the anonymous referee for carefully reading the manuscript, and D. S. thanks E. Treister for helpful discussion regarding models of AGN number counts in the mid-infrared. C. S. K. thanks R. Pogge for an introduction to Seyfert galaxy identification. This work is based on observations made with the *Spitzer Space Telescope*, which is operated by the Jet Propulsion Laboratory, California Institute of Technology, under NASA contract 1407. Support for this work was also provided by NASA through contract 1256790 issued by JPL/Caltech. Spectroscopic observations reported here were obtained at the MMT Observatory, a joint facility of the Smithsonian Institution and the University of Arizona. This work also made use of images and/or data products provided by the NDWFS, which is supported by the National Optical Astronomy Observatory (NOAO). NOAO is operated by the Association of Universities for Research in Astronomy (AURA), Inc., under a cooperative agreement with the National Science Foundation.

REFERENCES

Andreani, P., Spinoglio, L., & Malkan, M. A. 2003, ApJ, 597, 759
Barger, A., Cowie, L. L., Mushotzky, R. F., & Richards, E. A. 2001, AJ, 121, 662
Becker, R. H., White, R. L., & Helfand, D. J. 1995, ApJ, 450, 559
Brand, K., et al. 2005, ApJ, 626, 723
Croom, S. M., Smith, R. J., Boyle, B. J., Shanks, T., Miller, L., Outram, P. J., & Loaring, N. S. 2004, MNRAS, 349, 1397
Cutri, R. M., Nelson, B. O., Kirkpatrick, J. D., Huchra, J. P., & Smith, P. S. 2001, in ASP Conf. Ser. 232, The New Era of Wide-Field Astronomy, ed. R. Clowes, A. Adamson, & G. Bromage (San Francisco: ASP), 78
Devriendt, J. E. G., Guiderdoni, B., & Sadat, R. 1999, A&A, 350, 381
Eisenhardt, P. R., et al. 2004, ApJS, 154, 48
Fabricant, D. G., Hertz, E. N., Szentgyorgyi, A. H., Fata, R. G., Roll, J. B., & Zajac, J. M. 1998, Proc. SPIE, 3355, 385
Fazio, G. G., et al. 2004, ApJS, 154, 10
Förster Schrieber, N. M. 2000, AJ, 120, 2089
Glikman, E., Gregg, M. D., Lacy, M., Helfand, D. J., Becker, R. H., & Brotherton, M. S. 2004, ApJ, 607, 60
Haas, M., Siebenmorgen, R., Leipski, C., Meusinger, H., Müller, S. A. H., Chini, R., & Schartel, N. 2004, A&A, 419, L49
Hatziminaoglou, E., et al. 2005, AJ, 129, 1198
Hornschemeier, A. E., et al. 2001, ApJ, 554, 742
Jannuzi, B. T., & Dey, A. 1999, in ASP Conf. Ser. 191, Photometric Redshifts and High-Redshift Galaxies, ed. R. Weymann et al. (San Francisco: ASP), 111
Kenter, A., et al. 2005, ApJ, submitted (astro-ph/0507615)
Lacy, M., et al. 2004, ApJS, 154, 166
Laurent, O., Mirabel, I. F., Charmandaris, V., Gallais, P., Madden, S. C., Sauvage, M., Vigroux, L., & Cesarsky, C. 2000, A&A, 359, 887
Magorrian, J., et al. 1998, AJ, 115, 2285
Moran, E. C., Filippenko, A. V., & Chornock, R. 2002, ApJ, 579, L71
Murray, S. S., et al. 2005, ApJ, submitted (astro-ph/0504084)
Norman, C., et al. 2002, ApJ, 571, 218

Pentericci, L., et al. 2003, A&A, 410, 75
Richards, G. T., Vanden Berk, D., Reichard, T. A., Hall, P. B., Schneider, D. P., SubbaRao, M., Thakar, A. R., & York, D. G. 2002, AJ, 124, 1
Rieke, G. H., et al. 2004, ApJS, 154, 25
Sajina, A., Lacy, M., & Scott, D. 2005, ApJ, 621, 256
Schmidt, M., & Green, R. F. 1983, ApJ, 269, 352
Stern, D., et al., 2002a, AJ, 123, 2223
———. 2002b, ApJ, 568, 71
Treister, E., et al. 2004, ApJ, 616, 123
Tremaine, S., et al. 2002, ApJ, 574, 740
Vanden Berk, D. E., et al. 2001, AJ, 122, 549
Werner, M. W., et al. 2004, ApJS, 154, 1
Wolf, C., Wisotzki, L., Borch, A., Dye, S., Kleinheinrich, M., & Meisenheimer, K. 2003, A&A, 408, 499
Worsley, M. A., et al. 2005, MNRAS, 357, 1281